Naval Research Laboratory

Washington, DC 20375-5320

NRL/MR/7120-99-8369

Rapid Geoacoustics Inversion Methods Used in LWAD98-2 Sea Test

ALTAN TURGUT

Acoustic Signal Processing Branch
Acoustic Division

April 12, 1999

REPORT DOCUMENTATION PAGE

Form Approved
OMB No. 0704-0188

1. AGENCY USE ONLY (*Leave Blank*)	2. REPORT DATE	3. REPORT TYPE AND DATES COVERED
	April 12, 1999	

4. TITLE AND SUBTITLE

Rapid Geoacoustic Inversion Methods Used in LWAD98-2 Sea Test

5. FUNDING NUMBERS

6. AUTHOR(S)

Altan Turgut

7. PERFORMING ORGANIZATION NAME(S) AND ADDRESS(ES)

Naval Research Laboratory
Washington, DC 20375-5320

8. PERFORMING ORGANIZATION REPORT NUMBER

NRL/MR/7120--99-8369

9. SPONSORING/MONITORING AGENCY NAME(S) AND ADDRESS(ES)

Office of Naval Research
Arlington, VA 22217-5660

10. SPONSORING/MONITORING AGENCY REPORT NUMBER

11. SUPPLEMENTARY NOTES

12a. DISTRIBUTION/AVAILABILITY STATEMENT

Approved for public release; distribution unlimited.

12b. DISTRIBUTION CODE

A

13. ABSTRACT (*Maximum 200 words*)

A concept for rapid environmental characterization of the sea bottom/subbottom has been successfully tested during the LWAD98-2 seatest. As a proof-of-concept test, inversion of statistical parameters of a Jackson/Turgut bottom/subbottom scattering model from backscatter data is performed. Seabed geoacoustic properties are also inverted from normal-incidence acoustic data. Results are in agreement with the previously reported geoacoustic data for the area. Iterative time-reversal techniques were also used to improve backscattered signal quality in an engineering trial. All the time-reversal hardware and software components functioned well except for the proper band-pass filtering of the received backscatter signal.

14. SUBJECT TERMS

Geoacoustic inversion
Time-reversal acoustics
Bottom scattering
Underwater acoustics

15. NUMBER OF PAGES

14

16. PRICE CODE

17. SECURITY CLASSIFICATION OF REPORT	18. SECURITY CLASSIFICATION OF THIS PAGE	19. SECURITY CLASSIFICATION OF ABSTRACT	20. LIMITATION OF ABSTRACT
UNCLASSIFIED	UNCLASSIFIED	UNCLASSIFIED	UL

NSN 7540-01-280-5500

Standard Form 298 (Rev. 2-89)
Prescribed by ANSI Std 239-18
298-102

OUTLINE

1) Introduction.....1
2) Jackson/Turgut bottom backscattering model.....1
3) Inversion of seabed geoacoustic properties from reflection data.....3
4) Experiment and data analysis.....3
   a) Inversion using backscatter data.....3
   b) Inversion using normal-incidence reflection data.....4
   c) Time reversal in bottom scattering measurements.....4
5) Summary.....5
6) Acknowledgements.....5
7) References.....5

RAPID GEOACOUSTIC INVERSION METHODS USED IN LWAD98-2 SEA TEST

1) Introduction

The characterization of bottom geoacoustic and statistical properties is required for accurate prediction of sonar performance in littoral waters. In many of the areas considered to be sites of future Navy operations little is known of the bottom composition, particularly at depths more than a meter into the bottom. The real-time capability of remotely estimating seabed geoacoustic and statistical properties is especially important for Navy vessels operating in forward areas over previously unsurveyed bottoms.

During the Littoral Warfare Advanced Development (LWAD) 98-2 sea test, the concept of rapid environmental characterization using broad-band pulses was tested off the southwest coast of Florida in February/March 1998. The experiment area was located in the Gulf of Mexico near the Southwest Florida shelf break (see Figure 1). In addition to NRL single-frequency (1.5, 2.0, 2.5, 3.0, 3.5, 4.0, and 4.5 kHz) monostatic scattering measurements, broad-band (1.5 to 4.5 kHz) pulses were used to invert geoacoustic and statistical properties at site SR2 (25 36.26N, 84 07.95W). The idea of retransmitting the portions of the scattered signal for the enhancement of signal returned from corresponding annular patches is also tested. This report briefly describes the inversion techniques and their usage in a series of proof-of-concept and engineering trials during the LWAD98-2 experiment. The next two sections describe a bottom backscattering model and a normal-incidence reflection model which were used for inverting geoacoustic and statistical properties from backscatter data. Experiment, data analysis, and results are discussed in Section 4. Finally a brief summary is given in Section 5.

2) Jackson/Turgut bottom backscattering model

Bottom backscattering strength, $S_b(\theta)$ is defined as the decibel equivalent of the sum of interface and volume scattering cross sections (Urick, 1983)

$$S_b(\theta) = 10\log_{10}\left[\sigma_{cr}(\theta) + \sigma_v(\theta)\right] \qquad (1)$$

where θ is the grazing angle, $\sigma_{cr}(\theta)$ and $\sigma_v(\theta)$ are dimensionless backscattering cross sections per unit solid angle per unit area due to interface roughness and volume scattering, respectively. Both cross sections are calculated using perturbation approximations, and corrections for shadowing and large-scale bottom slope are included in the context of the composite roughness approximation (McDaniel and Gorman, 1983)

$$\begin{aligned} \sigma_{cr}(\theta) &= S(\theta,s)F(\theta,\sigma_{pr},s) \\ \sigma_v(\theta) &= S(\theta,s)F(\theta,\sigma_{pv},s) \end{aligned} \qquad (2)$$

where $S(\theta)$ is the shadowing correction, $F(\theta,\sigma,s)$ is a slope averaging integral, and s is the rms slope. A detailed evaluation of shadowing correction and rms slope averaging

Manuscript approved March 23, 1999.

integral can be found in the APL-UW Technical Report-9407 (1994). The bottom backscattering cross-section $\sigma_{pr}(\theta)$ in the Rayleigh-Rice approximation is given as (Kuo, 1963)

$$\sigma_{pr}(\theta) = 4k'^4 \sin^4\theta \left|Y(\theta)\right|^2 W(2k'\cos\theta) \tag{3}$$

where k' is the acoustic wavenumber in the water. The complex function $Y(\theta)$ is defined as

$$Y(\theta) = \frac{(q-1)^2\cos\theta + q^2 - \tau^2}{\left[q\sin\theta + \left(\tau^2 - \cos^2\theta\right)^{1/2}\right]^2} \tag{4}$$

where $q = \rho_0 / \rho_f$ is the ratio of the density of the sediment to the density of the water, $\tau = (1+i\delta)/v$ is the ratio of the complex wavenumber in the sediment to the real wavenumber in the water, δ is the loss parameter, and $v = c_0 / c_f$ is the ratio of the sediment sound velocity to water sound velocity. In the volume scattering model of Turgut (1998), after including refraction and transmission loss at the interface, volume scattering strength as a function of grazing angle is written as

$$\sigma_{pv}(\theta) = \frac{\eta \mathrm{Y} T(\theta)^2 \sin^2\theta}{2\sin\theta_r} \tag{5}$$

where $\eta = \left[4\pi\mathrm{Y} + \mathrm{Im}(k)\right]^{-1}$ is the inverse attenuation coefficient, θ_r is the refracted angle in the sediment, and Y is the volume scattering cross section. Two-way transmissivity $T(\theta)$ in the above equation is defined as

$$T(\theta) = \frac{4qv\sin\theta\sin\theta_r}{\left(qv\sin\theta + \sin\theta_r\right)^2} \tag{6}$$

Considering a transversely isotropic structure of sediment with sound-speed inhomogeneities having von Karman type of spectrum, the resulting volume scattering cross section can be written as

$$Y = \frac{k^4 a^2 b V_{\kappa\rho}^2 \mu_r}{2\sqrt{\pi}} \frac{\Gamma(m)}{\Gamma(m-3/2)} \left[1 + 4k^2\left(a^2\cos^2\theta_r + b^2\sin^2\theta_r\right)\right]^{-m}, \qquad m > 3/2, \tag{7}$$

where a where is the horizontal scale factor, b is the vertical scale factor, Γ is the Gamma function, and m is the spectral exponent. The parameter $V_{\kappa\rho}$ is defined as

$$V_{\kappa\rho} = -2\left(\frac{\gamma_\rho - \gamma_\kappa}{\gamma_\rho + \gamma_\kappa - 2}\right) \tag{8}$$

where $\gamma_\rho = \rho_r / \rho_0$ is the ratio of the grain density to the bulk sediment density and $\gamma_\kappa = \kappa_r / \kappa_0$ is the ratio of the grain compressibility to the bulk sediment compressibility.

3) Inversion of seabed geoacoustic properties form reflection data

As a forward model, the seabed is modeled as porous homogenous layers and the wavefield is conveniently decomposed into upgoing and downgoing waves within each

homogeneous layer. A matrix equation relates the upgoing and downgoing waves at the bottom interface of layer i to the upgoing and downgoing waves at the top of layer i+1 as

$$\begin{pmatrix} U'_i \\ \\ D'_i \end{pmatrix} = \begin{pmatrix} T'_i - \dfrac{R_i R'_i}{T_i} & \dfrac{R_i}{T_i} \\ -\dfrac{R'_i}{T_i} & \dfrac{1}{T_i} \end{pmatrix} \begin{pmatrix} U_{i+1} \\ \\ D_{i+1} \end{pmatrix} \tag{9}$$

where R_i,T_i are the reflection and transmission coefficients at interface i for waves that are incident above and R'_i,T'_i are the reflection and transmission coefficients for waves that are incident from below. The details of the derivation of seiosmogram equations for a layered poro-viscoelastic medium can be found in Turgut and Yamamoto (1988).

A previously developed time-domain inversion algorithm (Turgut and Wolf, 1996) was used for inverting seabed geoacoustic properties from normal-incidence reflection data. First, envelope functions of the matched-filtered acoustic returns are calculated by taking the absolute values of the acoustic returns in the form of analytic signals. The matched filtering achieves a signal processing gain over the background noise and provides compressed matched filter output. Then, instantaneous frequencies are calculated for a crude estimation of attenuation profile by comparing the center frequency shift in the acoustic return with that predicted by using the poro-viscoelastic attenuation model. Assuming an average sound speed value (1500 m/s) in the water column, water depth is calculated from the delay time between the transmission peak and the first return peak. Next, porosity, shear modulus, and permeability are inverted for the first sediment layer by using a global search algorithm within a model space. The model space is further constrained by well-established semi-empirical relations among the model parameters such as porosity, shear modulus, and attenuation. Random perturbations are applied to corresponding model parameters to minimize an objective function (quadratic deviation between the data and calculated synthetic seismogram for the first reflector). Acoustic parameters such as compressional speed and density are also calculated from the inverted model parameters using the poro-viscoelastic theory.

4) Experiment and Data Analysis

a) Inversion Using backscatter data

The monostatic scattering data were collected by using an existing NRL bottom-backscattering system. The NRL bottom backscattering system uses a USRD-G81 transducer as a source (source level 187 dB re 1 μPa @ 1m) and two 16-element hardened hydrophone arrays with 0.15 m element spacing. Prior to the experiment, several wideband (1.5 kHz to 4.5 kHz) 50 ms duration LFM waveforms were designed and digitally stored on a personal computer equipped with a digital-to-analog conversion board. A transmission schedule was designed for each site based on the source/receiver depth and water depth. Typically, 50 ms 10-25% cosine tapered waveforms were

transmitted every 15 s, allowing a sufficient decay of the reverberation tail. The backscattering strength was calculated by using the relation $S_b = 10\log_{10} M_b$, where the scattering coefficient M_b is given as (Bunchuk and Zhitkovskii, 1980)

$$M_b = \frac{I_s}{I_0}\frac{R^3}{\pi c_w \tau R_0^2}. \qquad (10)$$

In the above equation, R is the distance from source to the insonified area at the water-sediment interface, c_w is the sound speed in water, I_0 is the intensity of the transmitted signal at a distance R_0 from the source, τ is the finite duration of the transmitted pulse, and I_s is the intensity of the scattered signal. Since the transmitted and scattered signals were recorded by the same hydrophone array without clipping, relative levels of I_s and I_0 were used in the backscattering calculations. In Figure 2, the backscatter levels are depicted as a function of time and steering angle, calculated from the beam-time data by using the above equation. The bottom and surface scattering begin at about 0.1 s with bottom scattering component being dominant due to a null in the upward direction of the source beam pattern. The backscatter levels for frequencies with 0.5 kHz windows are also shown in Figure 2. The comparable bottom scattering levels for each frequency band indicate minor frequency dependency for this site. The backscattering levels were also comparable with those of the recently reported single-frequency backscattering scattering analysis (Kunz, 1998). Table 1 shows the geoacoustical and statistical parameters of the site SR2 area estimated from the backscattering data at 3 kHz. The corresponding *a posteriori* probability density (PPD) functions are plotted in Figure 3 with the mean and one standard deviation of the estimation. PPDs are good indicators of importance and uniqueness of each parameter. The estimated geaoacoustic and statistical parameters indicate the presence of typical sandy bottom in the area. Figure 4 shows the measured backscattering data and the model prediction using the inverted parameters. Notice that the model predictions are usually within an assumed 3-dB measurement error.

b) Inversion of normal-incidence reflection data

The seabed geoacoustic properties such as compressional speed, density, and attenuation are also estimated by using matched-filtered and endfire-beamformed data. Figure 5 shows matched filter output of direct and bottom reflected arrivals by steering the array in both end-fire directions. Notice that amplitude of direct signal is about four times larger than that of first bottom reflected signal (after the removal of geometrical spreading). A strong second signal right after the bottom return indicates a 2-3 m thick sediment layer overlying a hard bottom (strong reflector). Figure 6 shows the instantaneous frequency and envelope function of the bottom reflected signal. The average center-frequency shift calculated from the instantaneous frequency is about 13 Hz/m which corresponds to sandy bottom in the Biot/Turgut attenuation model (Turgut, 1998). For comparison, model prediction of the center frequency shift is given in Table 2 for different types of sediments. Figure 7 shows inverted compressional speed and density profiles for the site SR2 location. The values are comparable to those of a geoacoustic model reported in Bucca and Fulford (1997). However, additional "ground truth" data such as sediment core

measurements are needed to validate the inversion method applied to NRL scattering system data.

c) Time reversal in bottom scattering measurements

Application of time reversal in the bottom backscattering measurements is expected to produce robust backscattering strength measurements since the correlations of the retransmitted signals are done automatically by the seabed itself (Clouet and Fouque, 1997). Thus, a reduction in the measurement errors and data collection at lower grazing angles are expected. The engineering trial of the time-reversal software/hardware system was satisfactory except for the insufficient filtering of the returned signal. In the retransmitted signals, the low-frequency noise levels were much higher then the bottom scattering signals preventing a comprehensive testing of the method itself. This deficiency has been removed by using better band-pass filters and the system (and the method) is planned to be tested in future sea trials.

5) Summary

Rapid environmental characterization of the sea bottom/subbottom using the NRL scattering system has been performed during the LWAD98-2 seatest. The statistical parameters of a Jackson/Turgut bottom/subbottom scattering model were estimated from the backscatter data. Seabed geoacoustic properties were also inverted from normal-incidence acoustic data. Results are in agreement with the previously reported geoacoustic data for the area indicating a 2-3 m thick sandy layer over a hard subbottom (coral rock). The engineering trial of a time-reversal backscattering system was satisfactory except for the insufficient filtering of the low-frequency noise. This deficiency has been removed and will be tested in a future sea trial. Also, the inversion methods should be further validated by comparing the results with high-resolution sediment coring data from an area where the bottom composition is well documented.

6) Acknowledgments

This work was supported by the Office of Naval Research. We thank Bruce Pasewark, Ray Soukup, and Richard Menis of the Naval research Laboratory for data collection and experimental design. Editorial help from Steve Wolf is also greatly appreciated.

7) References

APL-UW High-Frequency Ocean Environmental Acoustic Handbook, Tech. Rep. APL-YW TR9407, AEAS 5501, Oct. 1994.

Bucca, P. J., and Fulford, J. K., "Environmental variability during the Littoral Warfare Advanced Development sponsored FTE 97-1 experiment," NRL Memorandum Report 7182—97-8048, Naval Research Laboratory, Washington, D.C., June 24, 1997.

Bunchuck, A. V. and Zhitkovskii Y. Y., "Sound scattering by the ocean bottom in shallow-water regions," Sov. Phys. Acoust., **26**(5), 1980.

Clouet, J. F., and Fouque, J. P., "A time-reversal method for an acoustical pulse propagating in randomly layered media," Wave Motion, 25, 361-368, 1997.

Kunz, E. L., "Bottom backscattering measured off the Southwest Coast of Florida during the Littoral Warfare Advanced Development 9802 experiment," NRL Memorandum Report 7140—98-8196, Naval Research Laboratory, Washington, D.C., September 4, 1998.

Kuo, E. Y., "Wave scattering and transmission at irregular surfaces," J. Acoust. Soc. Am. **36**, 2135, 1964.

McDaniel, S. T., and Gorman, A. D., "An examination of the composite roughness scattering model," J. Acoust. Soc. Am. **73**, 1476-1486, 1983.

Turgut, A., and Yamamoto, T., "Synthetic seismograms for marine sediments and determination of porosity and permeability," Geophysics, **53**(8), 1988.

Turgut, A., " Measurements of scattering due to sea bottom roughness and sub-bottom sound speed fluctuations", J. Acoust. Soc. Am., **90**(4), Pt.2, 22331, 1991.

Turgut, A. and Wolf, S. N., "Determination of seabed statistical properties and their effects on wave propagation in shallow water", J. Acoust. Soc. Am., **98**(5), Pt. 2, 2972, 1995.

Turgut, A., " Inversion of bottom/subbottom statistical parameters from acoustic backscatter data," J. Acoust. Soc. Am. **102**(2), 833-852, 1997.

Turgut, A., " Approximate expressions for viscous attenuation in marine sediments," (submitted to J. Acoust. Soc. Am., 1998).

Urick, R. J., *Principles of Underwater Sound,* (McGraw-Hill, New York), 1983.

Surface spectral exponent	(γ)	3.6245 (+/-0.2101)
Surface spectral strength	(β)	0.0066 (+/-0.0010)
Loss parameter	(δ)	0.0159 (+/-0.0016)
Aspect ratio	(α)	5.7949 (+/-0.3895)
Vertical scale factor	(b)	0.2269 (+/-0.1322)
Sound speed variance	(μ)	0.0170 (+/-0.0029)
Sound speed ratio	(ν)	1.1301 (+/-0.0115)
Volume spectral exponent	(m)	1.7342 (+/-0.0997)

Table 1. Inverted geoacoustic and statistical parameters from 3 kHz backscatter data. One standard deviation of the estimation are given in parentheses.

	Frequency shift (Hz/m)			
	$\delta=0.02$	$\delta=0.05$	$\delta=0.1$	$\delta=0.2$
Silty Clay	*0.67*	*0.88*	*1.15*	*1.69*
Clayey Silt	*1.28*	*1.48*	*1.75*	*2.43*
Silty Sand	*8.54*	*8.73*	*9.10*	*9.79*
Fine Sand	*14.57*	*14.81*	*15.17*	*15.95*

Table 2. Center Frequency shift for a 1.5-4.5 kHz signal estimated by Biot/Turgut sediment attenuation model for different frame loss coefficient (δ).

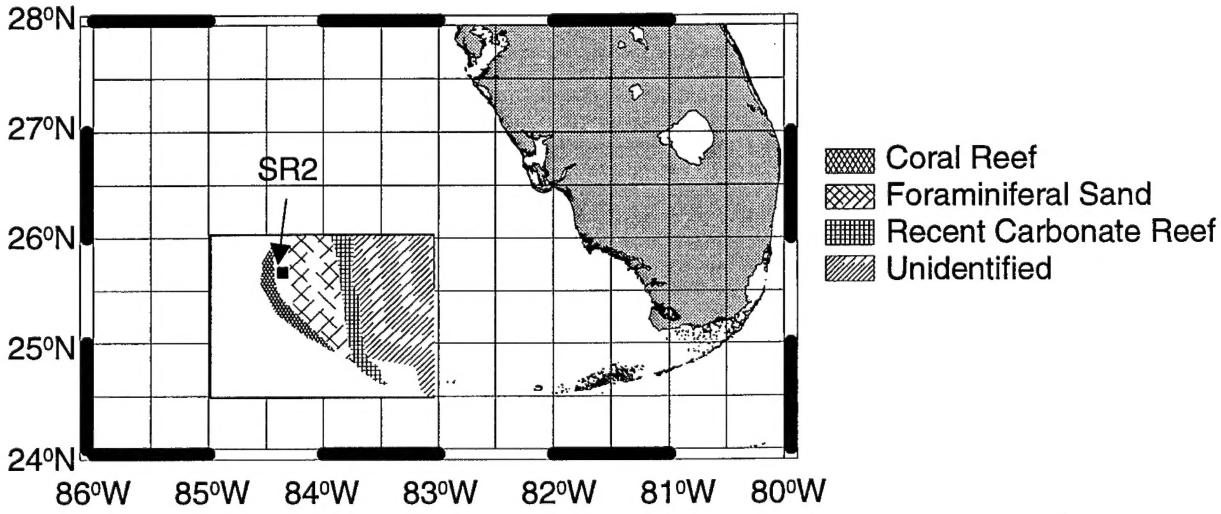

Figure 1. Location and bottom composition of LWAD98 bottom scattering experiment site SR2.

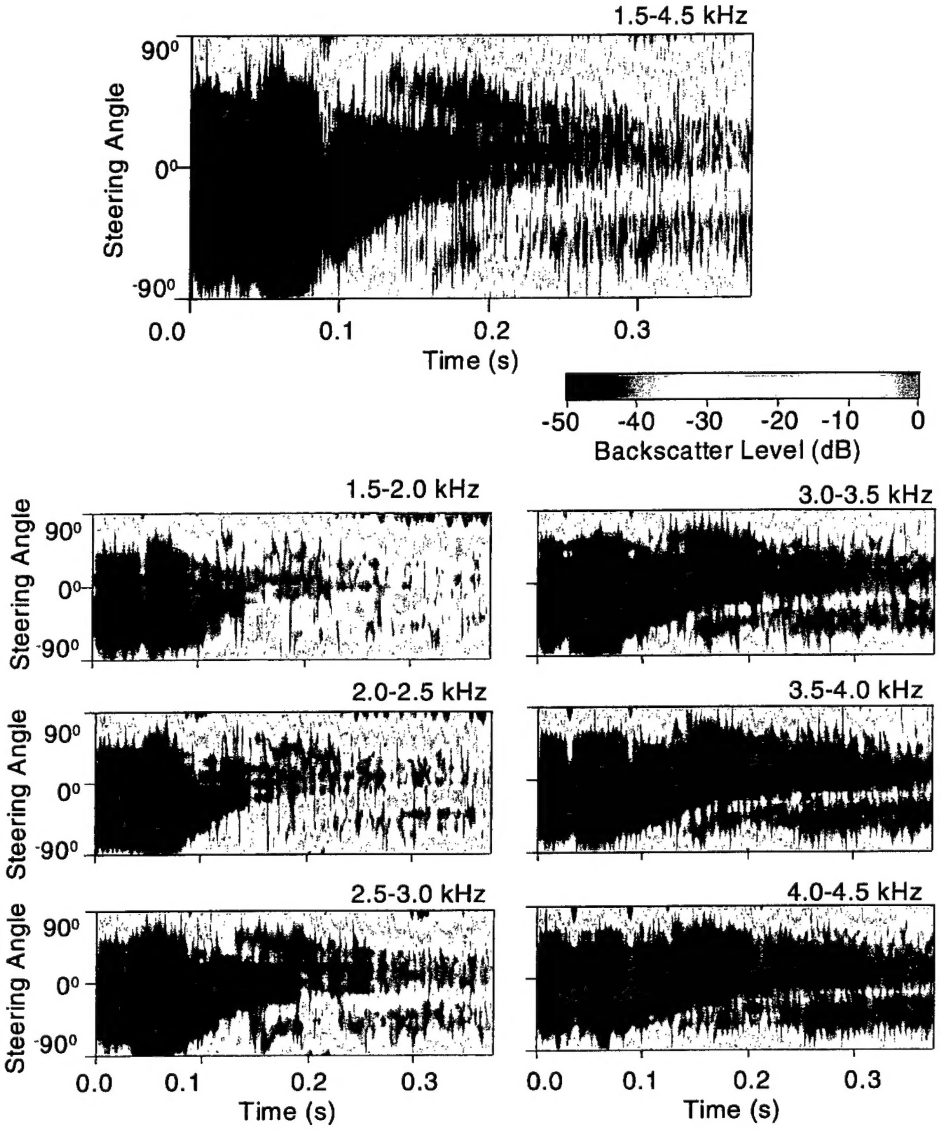

Figure 2. Measured backscatter levels as a function of time and steering angle.

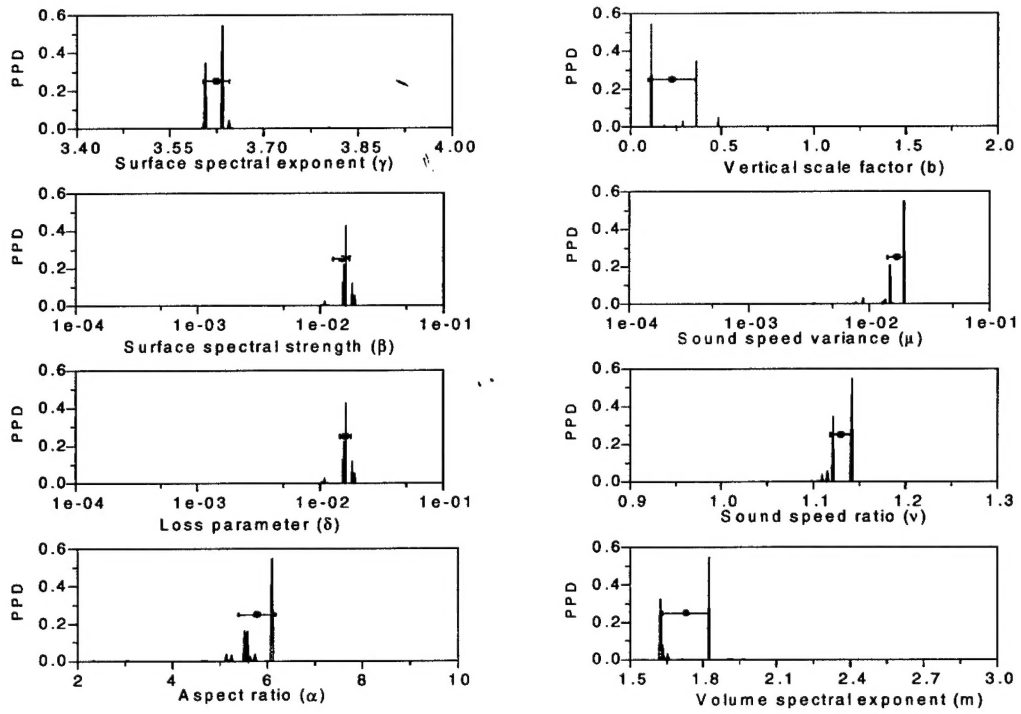

Figure 3. *A posteriori* probability density functions of geoacoustic and statistical parameters inverted for the SR2 site. The mean and one standard deviation of the estimation are also shown.

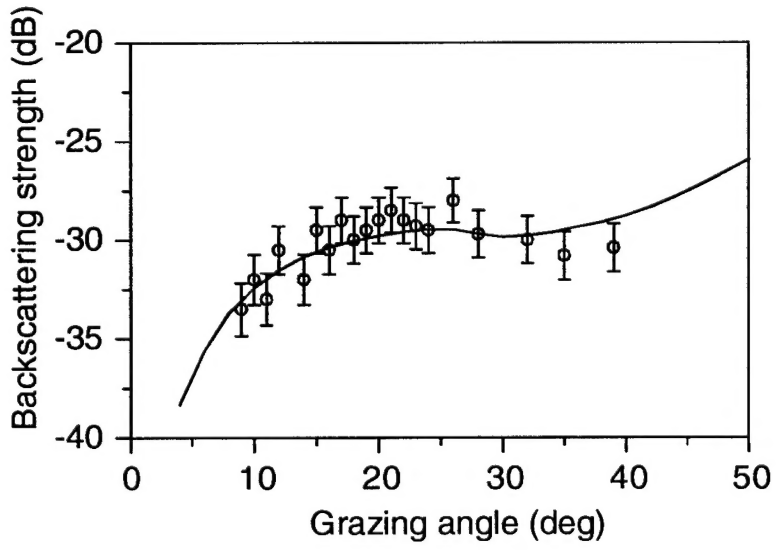

Figure 4. Measured backscattering data and model prediction using inverted parameters.

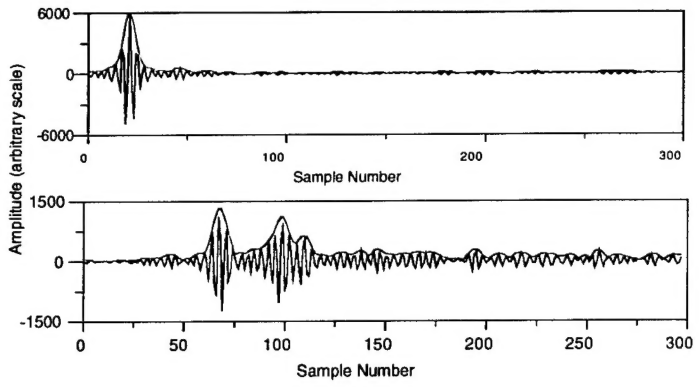

Figure 5. A typical matched filter output of endfire beamformed data

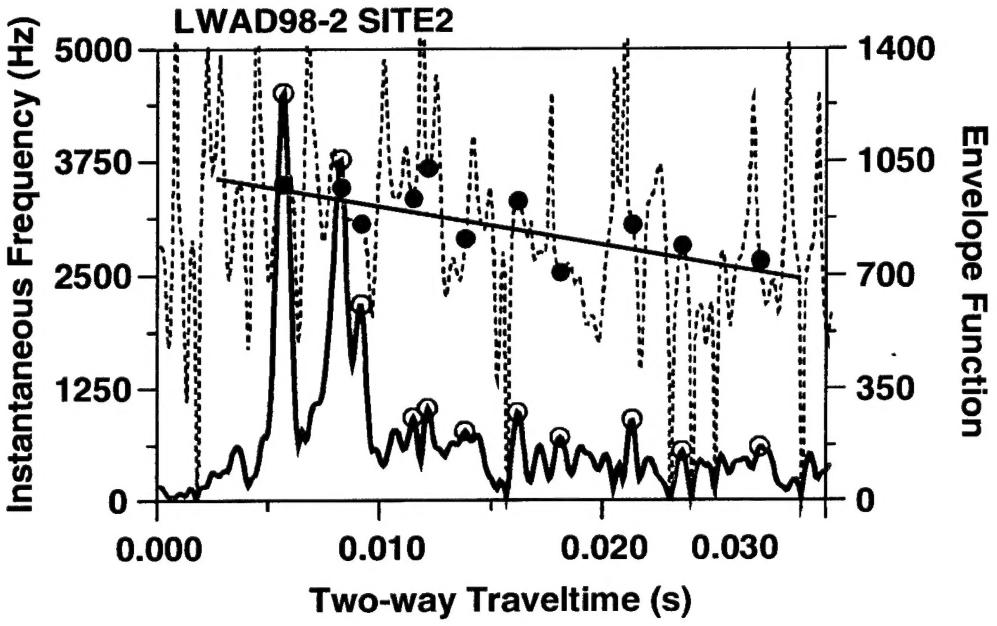

Figure 6. Instantaneous frequency (dotted line) and envelope function (solid line) for the average attenuation estimation. Regression line indicates a ~13 Hz/m center frequency shift. Dots indicate relatively high signal strength data selected for regression analysis.

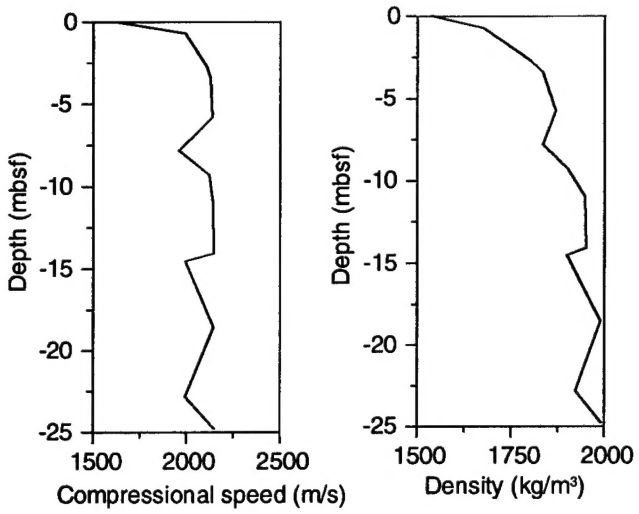

Figure 7. Estimated compressional wave speed and density profiles at the SR2 site. Depth unit is in meters below seafloor.